Line mixing and state-to-state rotational relaxation rates in D_2 determined from the Raman Q branch

P. M. Sinclair, J. W. Forsman, J. R. Drummond,* and A. D. May*
Department of Physics, University of Toronto, Toronto, Ontario, Canada M5S 1A7
(Received 29 January 1993)

Precise line-shape measurements of the $Q(0)$ to $Q(4)$ lines in D_2 have been made using Raman gain spectroscopy. At the densities studied (2.5–30 amagat), the Q-branch lines are well separated but slightly asymmetric due to quantum-mechanical line mixing. We have measured both the symmetric and the asymmetric contributions to the line shape as a function of the density. From the broadening coefficients and the line-mixing parameters, we have deduced the dephasing and the state-to-state rotational relaxation rates. Semiquantitatively, the results support the empirical modified-exponential-gap law.

PACS number(s): 33.70.Jg, 34.50.Ez, 34.50.Pi

INTRODUCTION

There has been much theoretical and experimental work done on line broadening and shifting in gases. At the pure physics level these studies have helped to elucidate the nature of intermolecular forces and collision dynamics. They have also been applied to a wide variety of topics including the interpretation of atomospheric data collected by remote sensing, and as a diagnostic tool in the study of hostile environments such as flames and combustion chambers.

There has been less work done on the problem of line mixing due to quantum-mechanical interference even though this effect can lead to profound changes in line shapes. While the broadening and shifting of an isolated line is described by a single diagonal element of the line relaxation matrix, the interference or mixing effects are due to a combination of the off-diagonal elements. For the isotropic component of the Raman Q branch, the off-diagonal elements of the relaxation matrix are, within a certain approximation, the state-to-state rotation relaxation rates [1].

Line mixing at very high densities has been studied extensively in HD [2–4] where it leads to collisional narrowing or collapse of the Q branch into a single narrowed band. It is clear that at high densities where the band becomes smooth and symmetric, any signature of specific state-to-state rates must be lost.

At intermediate densities, line mixing can cause an order of magnitude difference in the microwindows (region between lines) from what would be expected on a purely line additive basis. This has been examined by Cousin *et al.* [5] and Bulanin *et al.* [6] in infrared rotational structure.

At still lower densities it has been shown theoretically that line mixing leads to asymmetric collision broadened lines [7]. Very recently Thibault *et al.* [8,9] examined the shift in the peak location due to this asymmetry, an effect quadratic in density, and were able to extract single line-mixing parameters. However, other quadratic density effects may contaminate the measured quantity [10,11]. The object of this paper is a direct measurement of line asymmetries in the Q branch of pure D_2 at room temperature. With some approximations, we then extract from the asymmetries and the ordinary or symmetric broadening both state-to-state rotational relaxation rates and the vibrational dephasing. While there have been a number of "*cw*" spectroscopic attempts at determining rotational relaxation and vibrational dephasing rates [12–16] they all depend upon using some empirical scaling law such as the exponential gap model [17]. That is not the case here. Pulse probe experiments [18–21] also determine relaxation rates. While free from the use of such scaling laws they are, nevertheless, complimentary as they are not sensitive to rotationally resonant or vibrational dephasing collisions.

The paper is divided into the following sections, a review of ideas behind the experiment, experimental procedures, results and discussion, and finally a summary.

BACKGROUND

A general introductory overview of collision broadening and shifting combined with examples and references to state of the art theoretical calculations has been given by Green [22]. Generally one works within the impact approximation in which it is assumed that the duration of a collision is much shorter than the time between collisions. Within that approximation, the total band profile may be written down formally. However, the numerical evaluation of the spectrum requires a daunting matrix inversion. Fortunately, at low density the intensity profile can be written in a convenient form, as first pointed out by Rosenkranz [7].

We specialize Rosenkranz's result to a Raman Q branch where the band profile may be written

$$I(\omega)=\sum_j N(j)\left\{\frac{W_{jj}}{(\omega-\omega_j)^2+(W_{jj})^2}+\frac{(\omega-\omega_j)Y_j}{(\omega-\omega_j)^2+(W_{jj})^2}\right\}. \quad (1)$$

If detailed balance is used, the line mixing parameter Y_j,

is given by

$$Y_j = 2 \sum_{n\,(\neq j)} \frac{W_{nj}}{(\omega_j - \omega_n)} . \quad (2)$$

Here W_{nj} is the real part of an off-diagonal element of the line relaxation matrix describing the collisional transfer of the optical coherence from line j to line n. The element W_{nj} is inherently a negative number and provided we neglect rotation vibration coupling can be thought of as $-R_{nj}$, the rate of relaxation from rotational state j to rotational state n [1,22]. The Raman frequencies ω_j and ω_n (not the frequencies of the lines) contain the usual line shifts or the imaginary part of W_{jj} and W_{nn} [5] while $N(j)$ is the relative population of molecules in the initial rotational state associated with line j. The relaxation matrix is proportional to the density of perturbers. For a pure gas, as is the case here, we shall write $W_{nj} = \rho W^0_{nj}$, etc., where ρ is the number density in amagat units. In this paper W^0_{jj}, the broadening coefficient, gives the half width at half maximum (HWHM) of line j and is measured in cm^{-1}/amagat.

It is evident from the expression for $I(\omega)$, the band profile, that each line j in the band is made up of a symmetric Lorentzian part describing ordinary broadening (and shifting) and an asymmetric (dispersive) part rising from the line mixing. As mentioned above, Thibault *et al.* [8,9] used the nonlinear shift with density, of the location of the peak of a line, to measure several Y_j in CO-He mixtures. Independently, we have recognized the importance of measuring the mixing parameters but have chosen to extract the value of $Y_j = \rho Y^0_j$ for each line j by fitting the intensity profile to the sum of a Lorentzian and dispersion curve. Thus, aside from technical details, the thrust of the two approaches is the same, namely to use some signature of the profile of a single line at low densities to determine the line-mixing parameter for that line. The broadening, shifting, and now line mixing for each line are key experimental parameters to be compared with theoretical calculations [23]. To date there does not appear to be a clear signature for measuring the imaginary or phase part of the off-diagonal elements in the relaxation matrix [24]. Presumably that would represent a fourth experimental line parameter.

EXPERIMENTAL DETAILS

The cw Raman gain spectrometer used to record the Q branch of D_2 has been described previously [25]. We emphasize here only the features of the experimental and modifications to the system which are especially pertinent to the present study. It follows from Eq. (1) that the absolute amplitude of the (dispersive) line-mixing term has a maximum value at the half-width point of the Lorentzian term. In D_2, at our highest density, the peak value of the mixing term is of the order of 0.01 (i.e., 1% of the amplitude of the Lorentzian component at the half-height position). Thus to measure the small asymmetric component of the line shape two conditions are necessary: (i) we must have a very high signal-to-noise (S/N) ratio, and (ii) we must have very low instrumental asymmetry. The first condition is easily met with our spectrometer where, in a single-pass cell, we typically achieve S/N ratios of about 1500 for the $Q(1)$ and $Q(2)$ lines of D_2 for a 1 s integration time. The second condition is more difficult to satisfy. There are three main spurious contributions to the instrumental asymmetry, induced focusing, drift in the beam overlap, and effects associated with strain birefringence in the cell windows.

Induced focusing is discussed in [25] where it was called "other focusing." In another context it is referred to as "two-color z focusing" [26]. As the origin of the effect is the dispersion associated with the Raman gain, this dispersion has the spatial profile of the single-frequency argon laser used to drive the Raman gain. Thus, for the probe beam, the gas acts like a very weak lens, positive or negative, depending upon the frequency of the probe relative to the frequency of line center. Recall that the pump beam is modulated so that the Raman signal may be observed using phase-sensitive detection. As induced focusing is driven by the pump beam, the size of the probe beam is modulated at the same frequency. Consequently, if part of the beam is obstructed, modulation of the beam diameter produces a modulation in the intensity reaching the detector which is indistinguishable from a true Raman signal. Changing sign at line center, this spurious signal can produce large asymmetries in the resulting line shape. The effect is most often seen when the detected beam overfills the detector or is "clipped" by some optical component between the detector and the Raman gain cell. We have solved this problem by careful alignment and using a diffuse scatterer in an integrating-sphere-type geometry. The use of an actual integrating sphere (Labsphere, 1 in. diameter) resulted in too much loss due to the high average number of reflections. In our latest design the beam is focused into a cavity where it strikes a diffusing plane inclined at 45°. Typically 95% of the light reaches the detector after one scatter. This design has three advantages: (i) we can tightly focus the beam into the cavity thereby making sure that all the beam enters the detector section; (ii) the integrating cavity eliminates signal variations arising from motion of the beam over the nonuniform detector surface; and (iii) we can operate at higher power without saturating the high-frequency response of the detector, as the output beam is spatially "flat topped" instead of Gaussian.

The second source of asymmetry is drift in the pump and probe beam overlap during a scan. This is mainly due to a change in pointing of the dye laser during a scan. As reported earlier [25] this was greatly reduced using two quadrant detectors to detect each beam position and piezoelectric controlled mirror mounts in a feedback system to correct for beam drift. We have made two minor modifications to significantly improve the initial overlap and to reduce the drift. Previously we used the reflection from the back surface of a quartz window at 45° to "pick off" the beam for the quadrant detectors. But if the reflected beams are overlapped using the quadrant detectors the transmitted beams, which go to the Raman cell, will not be overlapped due to dispersion in the quartz window. In the past we used a compensating plate to overcome this problem. We find the use of a beam-

splitting cube is more convenient as it does not require a compensating plate or critical alignment. Our second modification has been a more judicious choice of location for the quadrant detectors. For each beam we have used lenses to image the first controlling mirror on the second quadrant detector and vice versa. This means that the first quadrant detector feedback system, for example, does not respond to beam corrections made by the second feedback system. We have also switched to gimbaled mirror mounts to further decouple the vertical and horizontal controls. As we shall see from our results, the use of a diffusive screen and the improvements to our "beam lock" system appears to have reduced the asymmetry from two-color z focusing to the point that it is small compared to the line-mixing asymmetries.

The third possible instrumental source of asymmetries is the residual birefringence in the cell windows. A slight depolarization of the pump and probe beams will introduce a small optically heterodyned Raman induced Kerr effect (RIKE) component to the signal. This asymmetric signal could be important in multipass cells [15]. It does not appear to be large in our single-pass system and if present is a constant over hours of operation, the time required to measure the asymmetry of a line at a number of densities.

OBSERVATIONS

As an example of the measured line profiles, Fig. 1 shows the $Q(2)$ line in pure D_2 at $32.0\pm0.1\,^{\circ}C$ and 22 amagat units of density. The dotted curve is a least-squares fitted curve made up of a Lorentzian and dispersive component and passes through the experimental points. Thirty times the dispersive component is shown as a dash-dotted curve. Deviations of the experimental points from a single Lorentzian (experiment minus Lorentzian) and from the compound or line mixing (experiment minus line mixing) fitted curve are shown, both multiplied by 30. If we take the rms deviations from a fitted curve as a measure of the noise then the signal to noise about the fits are 500 and 1100, respectively. Clearly the mixing model gives a better fit. Contrary to intuition, the deviation (experiment minus Lorentzian) does not reproduce the dispersive component when a "best fit" is sought by varying both the width and the center frequency of a pure Lorentzian curve.

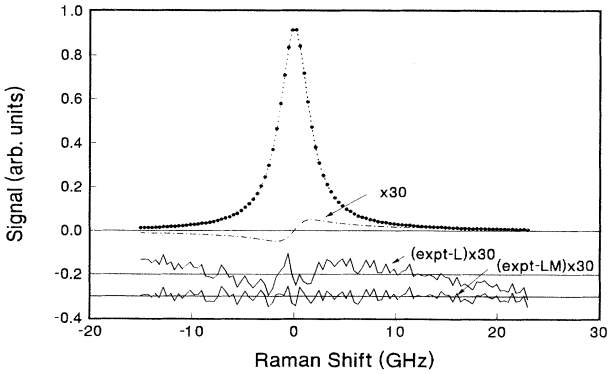

FIG. 1. The $Q(2)$ line of D_2 at 22 amagat and 32 °C. The dashed curve is the best-fit line-mixing line profile. The dash-dotted curve shows the asymmetric component.

From fits to experimental profiles we should be able, in principle, to extract information about broadening, shifting, line mixing, and the translational motion or Dicke narrowing [27,28]. Except for the very lowest densities, Dicke narrowing makes a negligible contribution to the width of the lines and need not concern us in this paper; we corrected for it using the soft-collision model [28]. The broadening and shifting measurements are part of a larger and inherently more precise study and will be reported in detail elsewhere. The measured mixing parameters are shown as a function of density in Fig. 2(a) for the ortho deuterium lines $Q(0)$, $Q(2)$, and $Q(4)$ and in Fig. 2(b) for the para deuterium lines $Q(1)$ and $Q(3)$. The scatter in the data for the strongest lines is of the order of 0.2% of the half-height of the Lorentzian component. The maximum amplitude of the mixing term occurs for the $Q(0)$ line and reaches a value of the order of 2% at the highest density. The weakest line for which we were able to measure an asymmetry was the $Q(4)$ line. This required us to average six scans of the line at each density. It is the average at each density that is shown for $Q(4)$. We believe the nonzero intercepts for all the lines are due to a RIKES signal introduced through a pressure-induced birefringence in the windows [15]; these

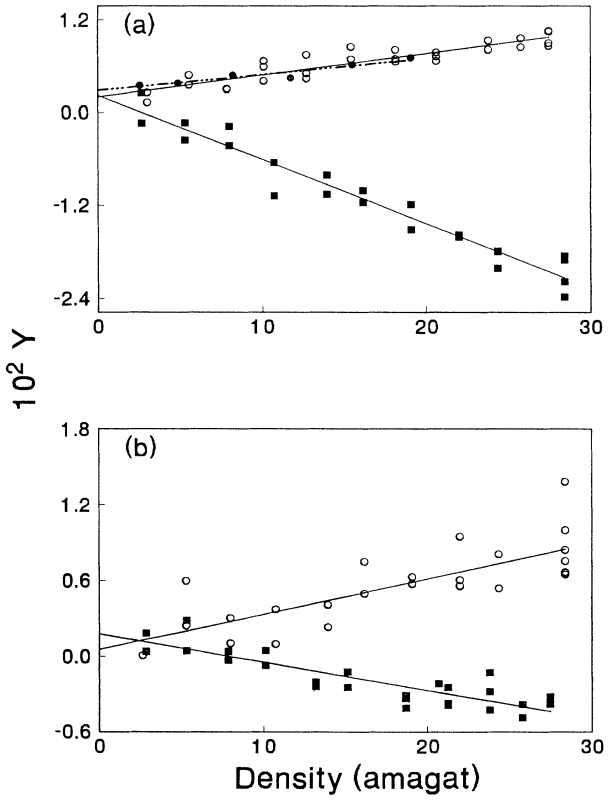

FIG. 2. The mixing parameters Y as a function of density. (a) Ortho deuterium: solid squares, $j=0$; open circles, $j=2$; solid circles, $j=4$. (b) Para deuterium: solid squares, $j=1$; open circles, $j=3$.

TABLE I. Mixing parameters and broadening coefficients in pure D_2.

Line	Mixing parameter (10^{-4} amagat^{-1})	Broadening coefficient (10^{-3} cm^{-1}/amagat)	
		This work	Smyth, Rosasco, and Hurst [14]
$Q(0)$	−8.3(5)	2.99(2)	2.97(9)
$Q(1)$	−2.2(3)	1.36(1)	1.33(4)
$Q(2)$	+2.8(3)	2.08(1)	2.06(6)
$Q(3)$	+2.8(5)	2.14(1)	2.13(6)
$Q(4)$	+2.1(6)	2.17(2)	2.15(6)
$Q(5)$		1.70(2)	1.71(9)
$Q(6)$		1.27(2)	

nonzero intercepts change slightly when the cell is pressure cycled. The slopes of the lines in Fig. 2, the Y_j^0's, are given in Table I along with our broadening coefficients (HWHM). Also included in the table are the broadening coefficients given by Smyth, Rosasco, and Hurst [14]. The two sets of broadening coefficients agree within experimental error.

Before proceeding with a detailed discussion of the results, it is worthwhile to point out the signatures that convinced us that the observed asymmetries are due to line mixing. Since the spin conversion rate is essentially zero one must think of the Q branch at room temperature as consisting of ortho deuterium lines and another independent set of para deuterium lines. Because of the quadratic spacing of the lines, then roughly speaking, $Q(0)$ and $Q(2)$ are one pair of interfering lines and $Q(1)$ and $Q(3)$ another pair [29]. As the effect of interference is to pull lines together, then from Eqs. (1) and (2) we expect Y_0^0 and Y_1^0 to be negative and Y_2^0 and Y_3^0 to be positive. This is precisely what is observed. If we add detailed balance to this argument, then roughly speaking we expect a Boltzmann relationship to hold. Thus we expect $-Y_0^0/Y_2^0$ to be equal to or greater than 2.2. [We say greater because the asymmetry of $Q(0)$ is enhanced and that of $Q(2)$ reduced by the presence of $Q(4)$.] The observed ratio is 3.0. For the para deuterium lines we expect $-Y_1^0/Y_3^0$ to be greater than or equal to 0.60. The observed ratio is 0.78. From these simple arguments we concluded that the observed asymmetries are due to line mixing. The following analyses leaves no doubt on this point [30].

We are not aware of any published theoretical values with which to compare our measured asymmetries. Thus we adopt a different approach if we are to analyze our results. Following the lead set by Smyth, Rosasco, and Hurst [14], or Rosasco *et al.* [15], *but without relying upon scaling laws,* we combine our experimental mixing parameters and broadening coefficients with Eq. (2) and a sum rule, to determine a number of W_{nj}^0's and the vibrational dephasing rate. Equation (2) involves an infinite number of W^0's and we have only a finite number of measured values of Y^0's. Detailed balance, $N(j)W_{nj}^0 = N(n)W_{jn}^0$, reduces the number of unknowns by a factor of 2. The sum rule $\sum_n W_{nj}^0 = W_{jj}^0 - \gamma$, where $n \neq j$ and $(S_{jj}^0 - \gamma)$ is the broadening of the $Q(j)$ line minus the vibrational dephasing contribution γ [1], adds another restriction and another unknown γ to the set of linear equations. To restrict the problem further we have tried two truncation schemes. In the first we limit the absolute change in the rotational quantum number to 2. In the second scheme we also allow an absolute change of 4. In both cases we included the broadening coefficient W_{66}^0 or W_{55}^0, one column beyond that for which a Y^0 was measured. The set of equations are overdetermined by one to three unknowns. Tables II and III give the least-squares fitted values of the components of the relaxation matrix along with the value of the dephasing rate for ortho and para deuterium, respectively. Actually, for the off-diagonal elements, we have tabled not W_{nj}^0 but rather $-W_{nj}^0$. This is for convenience when we talk about rotational state-to-state relaxation rates. The diagonal elements are the W_{jj} or the broadening coefficients minus γ. The first entry for a matrix element corresponds to allowing only $\Delta j = \pm 2$ transitions, the second entry for $\Delta j = \pm 2$ or ± 4. The third entry was calculated from the results of Smyth, Rosasco, and Hurst [14]. The entries at the top of each table for the fitted dephasing rate are in the same order as for the entries for an element of the matrix. A blank entry means the element was assumed to be zero. Some of the values have large uncertainties (W_{26} has an uncertainty of 10 times its value). However, we have resisted the temptation either to massage the

TABLE II. Ortho relaxation rates $-W_{nj}$ or W_{jj} in pure D_2, in 10^{-3} cm^{-1}/amagat. Vibrational dephasing, 0.54(04), 0.49(17),0.51(19) (10^{-3} cm^{-1}/amagat).

n \ j	0	2	4	6
0	2.45(04)	1.14(02)		
	2.50(17)	1.17(10)	0.00(32)	
	2.45[a]	1.13	0.17	
2	2.45(05)	1.54(04)	1.58(04)	
	2.50(21)	1.59(17)	1.66(26)	0.48(550)
	2.36	1.46	1.38	0.12
4		0.39(01)	1.63(04)	0.73(04)
	0.00(17)	0.41(07)	1.68(17)	0.30(550)
	0.08	0.33	1.60	0.78
6			0.05(00)	0.73(04)
		0.01(09)	0.02(35)	0.78(17)
		0.00	0.05	0.92

[a]See Ref. [14] for a discussion of uncertainties.

TABLE III. Para relaxation rates $-W_{nj}$ or W_{jj} in pure D_2, in 10^{-3} cm^{-1}/amagat. Vibrational dephasing 0.51(03),0.31(16),0.51(19) (10^{-3} cm^{-1}/amagat).

n \ j	1	3	5
1	0.85(03)	1.48(04)	
	1.05(16)	1.75(22)	0.75(59)
	0.87[a]	1.56	0.18
3	0.84(02)	1.63(03)	1.19(04)
	0.99(12)	1.83(16)	0.64(43)
	0.85	1.68	1.06
5		0.15(01)	1.19(03)
	0.05(04)	0.08(05)	1.39(16)
	0.011	0.12	1.26

[a]See Ref. [14] for a discussion of uncertainties.

data or to look for a better truncation scheme. The latter should be attempted when there are theoretical values available to justify neglecting specific terms. The present analysis is sufficient for the moment. For ortho deuterium our two sets of values, obtained with different truncations, overlap. This is not strictly true for the para deuterium case but the two sets of numbers are, in general, close. We see that the $(j+4\leftarrow j)$ rates are much smaller than the $(j+2\leftarrow j)$ rates. Thus our experiment confirms what has long been known from theory, that the rotational relaxation in D_2 is dominated by $\Delta j=\pm 2$ transitions. Because of this, the values of the $\Delta j=\pm 2$ rates are relatively insensitive to the truncation procedure. Since we assumed that the dephasing rate was j independent it is gratifying that the average of the two values of γ determined for ortho deuterium, 0.54(4)/0.49(17), and para deuterium, 0.51(3)/0.31(16), are nearly the same within experimental uncertainties.

While the results above were obtained directly from the experimental results without recourse to any energy gap model, it is interesting nevertheless to compare our rate analyses with that of Smyth, Rosasco, and Hurst [14]. They determined state-to-state rotational relaxation rates at 24±1 °C using only measured broadening coefficients for $Q(0)$ to $Q(5)$ and an exponential-gap model [31]. The model contained a constant dephasing rate and three adjustable rate parameters. They found a dephasing rate of $0.51(19)\times 10^{-3}$ cm^{-1}/amagat, which is not inconsistent with our values. Using their constants for D_2 at room temperature yielded the components of the state-to-state relaxation matrix shown as the third entries in the tables. (The diagonal elements were determined using the sum rule.) The close agreement between either of our values and their values represents a test and semiquantitative confirmation of the empirical scaling law.

There have been other experiments to measure the rotational relaxation rates. As noted by Smyth, Rosasco, and Hurst, the pump probe experiments of Meier, Ahlers, and Zacharias [19] are completely inconsistent with the measured broadening. Their rates would violate the sum rule.

SUMMARY AND CONCLUSIONS

We have directly measured the line-mixing coefficients in D_2 at room temperature and low densities. These can be compared with close-coupled calculations when they become available. Thus line mixing at low densities provides us with an additional spectroscopic technique whereby relaxation processes may be measured or theories tested. With some reasonable assumptions we have analyzed the asymmetries to deduce rotational state-to-state rates ($-W_{nj}$) and the vibrational dephasing rate. The state-to-state rates are in semiquantitative agreement with the rates calculated from an exponential-gap model with parameters adjusted to fit the broadening data alone.

ACKNOWLEDGMENTS

The authors gratefully acknowledge the support of the Natural Science and Engineering Research Council of Canada and the Province of Ontario through the Ontario Laser and Lightwave Research Centre. J.W.F. and P.M.S. gratefully acknowledge the support the Walter C. Sumner Memorial Fund.

*Also at the Ontario Laser and Lightwave Research Centre, Toronto, Canada.

[1] B. Lavorel, G. Millot, J. Bonamy, and D. Robert, Chem. Phys. **115**, 69 (1987).
[2] P. Dion and A. D. May, Can. J. Phys. **51**, 36 (1973).
[3] T. Witkowicz and A. D. May, Can. J. Phys. **54**, 575 (1976).
[4] J. Bonamy, L. Bonamy, and D. Robert, J. Chem Phys. **67**, 4441 (1977).
[5] C. Cousin, R. Le Doucen, C. Boulet, A. Henry, nd D. Robert, J. Quant. Spectrosc. Radiat. Transfer. **36**, 521 (1985).
[6] M. O. Bulanin, A. B. Dokuchaev, M. V. Tokov, and N. N. Filippov, J. Quant. Spectrosc. Radiat. Transfer. **31**, 521 (1984).
[7] P. W. Rosenkranz, IEEE Trans. Antennas Propag. **AP-23**, 498 (1975).
[8] F. Thibault, J. Boissoles, R. Le Doucen, R. Farrenq, M. Morillon-Chapey, and C. Boulet, J. Chem. Phys. **97**, 4623 (1992).
[9] F. Thibault, J. Boissoles, R. le Doucen, and C. Boulet, Europhys. Lett. **12**, 319 (1990).
[10] A. D. May, V. Degen, J. C. Stryland, and H. L. Welsh, Can. J. Phys. **39**, 1769 (1961).
[11] A. Royer, Phys. Rev. A **22**, 1625 (1980).
[12] L. A. Rahn and R. E. Palmer, J. Opt. Soc. Am. B **3**, 1164 (1986).
[13] M. L. Koszykowski, L. A. Rahn, R. E. Palmer, and M. E. Coltrin, J. Phys. Chem. **91**, 41 (1987).
[14] K. C. Smyth, G. J. Rosasco, and W. S. Hurst, J. Chem. Phys. **87**, 1001 (1987).
[15] G. J. Rosasco, A. D. May, W. S. Hurst, L. B. Petway, and K. C. Smyth, J. Chem. Phys. **90**, 2115 (1989).

[16] L. A. Rahn, R. L. Farrow, and G. J. Rosasco, Phys. Rev. A **43**, 6075 (1991).
[17] J. I. Steinfeld, P. Ruttenburg, G. Millot, G. Fanjoux, and B. Lavorel, P. Phys. Chem. **95**, 9638 (1991).
[18] D. W. Chandler and R. L. Farrow, J. Chem. Phys. **85**, 810 (1986).
[19] W. Meier, G. Ahlers, and H. Zacharias, J. Chem. Phys. **85**, 2599 (1986).
[20] R. L. Farrow and D. W. Chandler, J. Chem. Phys. **89**, 1994 (1988).
[21] G. O. Sitz and R. L. Farrow, J. Chem. Phys. **93**, 7883 (1990).
[22] S. Green, *Status and Future Development in Transport Properties,* edited by W. A. Wakeham *et al.* (Kluwer Academic, Dordrecht, 1992).
[23] E. W. Smith, J. Chem. Phys. **74**, 6658 (1981).
[24] J. Boissoles, C. Boulet, D. Robert, and S. Green, J. Chem. Phys. **90**, 5392 (1989).
[25] J. W. Forsman, P. M. Sinclair, P. Duggan, J. R. Drummond, and A. D. May, Can. J. Phys. **69**, 558 (1991).
[26] M. Sheik-Bahae, J. Wang, R. DeSalvo, D. J. Hagan, and E. W. Van Stryland, Opt. Lett. **17**, 258 (1992).
[27] J. W. Forsman, P. M. Sinclair, A. D. May, P. Duggan, and J. R. Drummond, J. Chem. Phys. **97**, 5355 (1992).
[28] L. Galatry, Phys. Rev. **122**, 1218 (1961); see also R. Blackmore, S. Green, and L. Monchick, J. Chem. Phys. **91**, 3846 (1989).
[29] While interference occurs only between ortho or para lines we do allow for the noninterfering but overlapping of Lorentzian components.
[30] There are other sources of line asymmetries, such as those in Ref. [11] or in the work of Ph. Marteau, C. Boulet, and D. Robert, J. Chem. Phys. **80**, 3632 (1984); and in the work of R. L. Farrow, L. A. Rahn, and G. O. Sitz, Phys. Rev. Lett. **63**, 746 (1989). In these cases, the asymmetry would be always on the same side of the Q-branch lines, in stark contrast to the reversal, from line to line, of the asymmetries observed here. The success of the analyses of our observations is convincing evidence that the *dominant* source of asymmetries in the present experiment is due to line mixing.
[31] This involves an additional assumption that the rotation-vibration coupling may be ignored [1,22]. As a consequence the rotational state-to-state relaxation rates are related to the relaxation matrix by $R_{nj} = -W_{nj}$.